



25<sup>th</sup> ABCM International Congress of Mechanical Engineering  
October 20-25, 2019, Uberlândia, MG, Brazil

**COB-2019-0654**

## **A NEW APPROACH FOR COMPUTING THE TOTAL ABSORPTIVITY OF NON-GRAY SURFACES IN RADIATIVE HEAT EXCHANGES WITH A PARTICIPATING MEDIUM**

**Roberta Juliana Collet da Fonseca**

**Guilherme Crivelli Fraga**

**Francis Henrique Ramos França**

Department of Mechanical Engineering, Federal University of Rio Grande do Sul – 425 Sarmento Leite St., Porto Alegre, Brazil

roberta.fonseca@ufrgs.br

guilhermecfraga@ufrgs.br

frfranca@mecanica.ufrgs.br

**Abstract.** *This paper proposes a new methodology based on a transmissivity-weighted average temperature of the medium to approximate the total hemispherical absorptivity of non-gray surfaces that bounded and exchange radiative heat with a participating gas. In this sense, this is an extension to a recent method to model the radiative transfer between non-gray surfaces and participating media. The new methodology is assessed for a set of one-dimensional test cases involving non-isothermal mixtures of water vapor and carbon dioxide. The gas properties are evaluated using line-by-line (LBL) spectral data, and the radiative transfer equation is solved through the discrete ordinates method. The accuracy of the proposed methodology is compared against other ways to estimate the total absorptivity of the surfaces, using as reference a solution that truly considers the surfaces to be non-gray. Results show that, as the temperature distribution in the medium gets less symmetric, the transmissivity-weighted average is in general more accurate than an older approach for computing the absorptivity, although the former formulation does not perform as well as others for roughly symmetric profiles. However, additional analyses showed that a possible improvement to this formulation can be achieved by taking into account the temperature of the boundaries when computing the absorptivity.*

**Keywords:** *thermal radiation, total absorptivity, line-by-line integration, non-gray walls, medium transmissivity*

### **1. INTRODUCTION**

Spectral modeling of participating media is a challenging subject in the thermal radiation area due to the difficulty to describe the highly complex dependence of the spectral absorption coefficient with the wavenumber, especially in problems that involve large variations of temperature and molar concentrations of the participating species (Modest, 2013; Howell *et al.*, 2016). Although it requires an elevated computational effort, the line-by-line (LBL) integration method provides a very accurate solution for these cases, since it accounts the contribution of each absorption line of the wavenumber spectrum. Alternatively, it is possible to have efficient, approximate solutions by using global spectral models, such as the weighted-sum-of-gray-gases (WSGG) (Modest, 1991) or the spectral-line based WSGG (SLW) (Denison and Webb, 1993) models, which solve directly for the total radiation intensity, being able to provide fairly accurate results with only a part of the time of a LBL solution.

When the participating medium is contained within enclosures with non-gray boundaries, the radiative transfer calculations get even more complex. Because global models are not capable of resolving spectral quantities, it is not possible to determine the spectral emissivity and absorptivity of the walls of the enclosure when prescribing the boundary conditions to solve the radiative transfer equation (RTE), so alternative approaches are necessary. Previous attempts to employ global models for calculations involving non-gray walls include those reported in Denison and Webb, 1994, Solovjov *et al.*, 2013, Fonseca *et al.*, 2018b, and Silva *et al.*, 2018, but they often require additional simplifications or incur in a significant increase in the computational cost. Recently, a new methodology has been proposed for this kind of problem (Fonseca *et al.*, 2018a), consisting in prescribing total absorptivity to the non-gray surfaces and solving the RTE as if the medium was bounded by gray surfaces. Although this methodology, named the global absorptivity approach (GAA), has shown to be capable of providing accurate results with moderate computational costs for both the WSGG and SLW models (Fonseca *et al.*, 2018a; Silva *et al.*, 2018), there is still no well-established procedure to determine the total absorptivity of the surfaces.

In this framework, this paper aims to propose and test a new way of estimating the total absorptivity to be used in the aforementioned GAA based on a transmissivity-weighted average over the entire domain. For simplicity, the calculations

are carried out for a one-dimensional participating medium slab bounded by non-gray surfaces with prescribed spectral emissivities. The medium consists of a non-isothermal mixture of carbon dioxide and water vapor, the radiative properties of which are determined from high-resolution line-by-line data. Different temperature profiles are considered, with an increasing degree of asymmetry. The accuracy of this new approach for computing the total absorptivity is compared to the one introduced by Fonseca *et al.*, 2018a, and to results of a calculation where the surfaces are exactly treated as non-gray.

## 2. RADIATION MODELING

### 2.1 The spectral RTE solved for media bounded non-gray boundaries

Assuming a participating medium in which the scattering effects can be neglected, the RTE along a given path  $s$  is calculated as (Modest, 2013; Howell *et al.*, 2016)

$$\frac{dI_\eta}{ds} = -\kappa_\eta I_\eta + \kappa_\eta I_{\eta b}, \quad (1)$$

where  $I_\eta$  is the spectral radiation intensity,  $\kappa_\eta$  is the spectral absorption coefficient of the medium, and  $I_{\eta b}$  is the blackbody spectral radiation intensity, obtained from the Planck's distribution function for a wavenumber  $\eta$  and a medium temperature  $T$ .

The boundary condition required for solving the Eq. (1) for an opaque, non-gray surface with spectral hemispherical emissivity  $\varepsilon$  and spectral absorptivity  $\alpha$  can be expressed as

$$I_{\eta,0} = \varepsilon_\eta I_{\eta b,0} + \frac{(1 - \alpha_\eta)}{\pi} G_\eta, \quad (2)$$

in which  $I_{\eta,0}$  and  $I_{\eta b,0}$  are the spectral intensity and spectral blackbody intensity at the boundary, the latter given as  $I_{\eta b,0} = I_{\eta b}(T_0)$ , with  $T_0$  the boundary temperature. The term  $G_\eta$  in the previous equation is the spectral hemispherical irradiation, determined as the incoming intensity  $I_{\eta,i}$  at the boundary integrated over all solid angles  $\omega$ ,  $G_\eta = \int_{2\pi} I_{\eta,i} \cos \theta d\omega$ , where  $\theta$  is the angle between the solid angle and the unit vector normal to the boundary. Note also that Kirchhoff's law dictates that  $\varepsilon_\eta = \alpha_\eta$  for opaque surfaces (Modest, 2013).

### 2.2 The global absorptivity approach

The global absorptivity approach (GAA) was first proposed by Fonseca *et al.*, 2018a, as a manner to simplify the solution of the radiative transfer in non-gray media bounded by non-gray walls when applying global spectral models such as the weighted-sum-of-gray-gases (WSGG) (Modest, 1991) or the spectral line-based WSGG (SLW) (Denison and Webb, 1993). However, here the method will be described in more broader terms, since, for testing purposes, in the present study it will be applied only in the framework of the line-by-line integration methodology. The GAA is based on solving the spectrally-integrated form of the RTE,

$$\frac{dI}{ds} = -\kappa_G I + \kappa_P I_b, \quad (3)$$

where  $I = \int_0^\infty I_\eta d\eta$  and  $I_b = \int_0^\infty I_{\eta b} d\eta$  are the total radiation intensity and total blackbody intensity, respectively,  $\kappa_G = \int_0^\infty \kappa_\eta I_\eta d\eta / I$  is the incident-mean absorption coefficient, and  $\kappa_P = \int_0^\infty \kappa_P I_{\eta b} d\eta / I_b$ . This equation is subjected to the following boundary condition:

$$I_0 = \varepsilon I_{b,0} + \frac{(1 - \alpha)}{\pi} G, \quad (4)$$

with the index 0 again indicating a quantity evaluated at the wall, and  $G = \int_0^\infty G_\eta d\eta$  the total hemispherical irradiation. In Eq. (4),  $\varepsilon$  and  $\alpha$  are the total hemispherical emissivity and absorptivity of the boundary, whose definitions can be derived by comparing this equation to Eq. (2). This results in

$$\varepsilon = \frac{\int_0^\infty \varepsilon_\eta I_{\eta b}(T_0) d\eta}{I_b(T_0)}, \quad (5)$$

$$\alpha = \frac{\int_0^\infty \alpha_\eta G_\eta d\eta}{G}. \quad (6)$$

It is important to note that, unless the participating medium is gray (i.e.,  $\kappa_\eta$  does not depend on  $\eta$ , yielding  $\kappa_G = \kappa_P$ ), the simultaneous solution of Eqs. (3) and (4) will not give out the same total radiation field as what would be obtained by

solving Eqs. (1) and (2) for  $I_\eta$  and then integrating on the spectrum, even if the exact definitions of  $\varepsilon$  and  $\alpha$  provided in Eqs. (5) and (6) were used. Nevertheless, previous tests demonstrated (and the present study will show this as well) that the approach given by Eqs. (3)–(6) is capable of very accurate predictions of the non-gray radiation field even for highly complex profiles of  $\varepsilon$ . However, this methodology suffers from a major setback: for determining  $\alpha$  in Eq. (6), it is necessary the knowledge of  $G_\eta$  and, as a consequence, of  $I_\eta$ , which in turn can only be obtained by solving the RTE in its spectral form.

With this in mind, Fonseca *et al.*, 2018a, introduced the concept of a reference medium temperature  $T_{rm}$ , whose value is defined as to approximately satisfy  $G_\eta \approx I_{\eta b}(T_{rm})$  when evaluating the hemispherical absorptivity of the non-gray boundaries. This let us rewrite Eq. (6) as

$$\alpha = \frac{\int_0^\infty \alpha_\eta I_{\eta b}(T_{rm}) d\eta}{I_b(T_{rm})}, \quad (7)$$

so that  $\alpha$  could be estimated in a similar fashion as the hemispherical emissivity (albeit using a temperature that would almost certainly be different from the boundary temperature), i.e., without the need of knowing the spectral irradiation.

The GAA allows for an efficient application of global models in the solution of the radiative heat exchange between participating media and non-gray surfaces, as it has already been shown in the framework of the WSGG model (Fonseca *et al.*, 2018a) and of the SLW model (Silva *et al.*, 2018). However, an accurate solution of the radiative transfer with the GAA can only be achieved if an adequate value for the reference temperature is chosen, since the presumed absorptivity estimated by Eq. (7) is dependent on  $T_{rm}$ . In the next section, the procedure adopted so far for obtaining  $T_{rm}$  is described, alongside the new methodology proposed in the present study.

### 2.3 Forms of defining the reference medium temperature

In Fonseca *et al.*, 2018a, and in Silva *et al.*, 2018, the reference medium temperature was defined as the domain-average temperature within the computational domain, i.e., for a one-dimensional medium of length  $L$ ,  $T_{rm}$  would be given as

$$T_{rm} = \frac{\int_0^L T(x) dx}{L}. \quad (8)$$

In the aforementioned papers, this method of determining the reference medium temperature was successfully applied to a series of one-dimensional radiative transfer calculations involving non-isothermal media with symmetrical temperature distributions. However, for a medium with a non-symmetrical  $T$ -profile, especially when the temperature of the boundaries is different one from the other, Eq. (8) may find have some difficulty in providing an adequate estimate for  $T_{rm}$ .

An alternative formulation for computing  $T_{rm}$  is proposed here, based on a domain-average of the temperature weighted by the transmissivity from any boundary to the medium,

$$T_{rm} = \frac{\int_0^L \tau_{0 \rightarrow x} T(x) dx}{\int_0^L \tau_{0 \rightarrow x} dx}, \quad (9)$$

in which  $\tau_{0 \rightarrow x}$  is total transmissivity for a path between the boundary and a position  $x$  within the medium. The total transmissivity for an isothermal and homogeneous medium (i.e., where the spectral absorption coefficient of the medium is constant throughout the path,  $\kappa_\eta = \bar{\kappa}_\eta$ ) is defined as

$$\tau_{0 \rightarrow x} = \frac{\int_0^\infty I_{\eta,0} \exp(-\bar{\kappa}_\eta x) d\eta}{I_0}. \quad (10)$$

To employ this equation in the non-isothermal cases presently studied,  $\bar{\kappa}_\eta$  is first defined as a domain-average value of the real absorption coefficient from the boundary until position  $x$ ,  $\bar{\kappa}_\eta = (1/x) \int_0^x \kappa_\eta(x') dx'$  (where  $x'$  is an arbitrary variable for the integration). This allows Eq. (10) to be rewritten to

$$\tau_{0 \rightarrow x} = \frac{\int_0^\infty I_{\eta,0} \exp\left(-\int_0^x \kappa_\eta dx'\right) d\eta}{I_0}, \quad (11)$$

which still requires the knowledge of the spectral radiation field to be solved. To simplify this expression and make it applicable to solutions with global spectral models, let's assume in Eq. (11) that the medium is gray; thus, both  $I_{\eta,0}$  and  $\kappa_\eta$  are independent on  $\eta$  and the spectral integration in that equation can be disregarded. Furthermore, let's also choose to evaluate  $\kappa$  with the Planck-mean absorption coefficient  $\kappa_P$  (see the discussion following Eq. (3)). This ultimately leads to

$$\tau_{0 \rightarrow x} = \exp\left(-\int_0^x \kappa_P dx'\right). \quad (12)$$

Equation (9) has the advantage of allowing that a different value of  $T_{rm}$  be used to predict the presumed  $\alpha$  of each boundary. For a one-dimensional medium with non-uniform properties, for instance, the transmissivity computed via either Eq. (11) or (12) can be different when it is calculated starting from the left or the right boundaries, yielding then different values of  $T_{rm}$  for those surfaces. Hopefully, this will lead to better results for the application of the GAA to highly non-uniform media.

In this study, five different forms of application of the GAA are evaluated. In all of them, Eq. (3) is solved via LBL integration subjected to the boundary condition given by Eq. (4), with the total hemispherical emissivity of the surfaces that bound the medium computed via Eq. (5). Furthermore, in all but one of the tested approaches, the presumed total hemispherical absorptivities of the surfaces are calculated via Eq. (7) and the only difference is in how the reference medium temperature is estimated. In the first formulation, GAA-1,  $T_{rm}$  is determined following the methodology proposed by Fonseca *et al.*, 2018a, and expressed by Eq. (8). In the second (GAA-2), Eq. (11) is adopted for  $T_{rm}$ , evaluating  $\kappa_\eta$  from the LBL absorption spectra and  $I_{\eta,0}$  and  $I_0$  from a separated calculation that considers the walls to be non-gray. The third and fourth formulations (GAA-3 and GAA-4, respectively) both employ Eq. (12), using the correlation for the Planck-mean absorption coefficient developed by Cassol *et al.*, 2015; the difference is that GAA-3 let the medium properties vary along the optical path, while GAA-4 assumes a constant  $\kappa_P$  throughout the path, evaluated from the average temperature and average medium composition. Finally, GAA-5, although applying the same idea of the GAA—i.e., solving Eqs. (3) and (4) instead of Eqs. (1) and (2)—does not estimate  $\alpha$  from a medium reference temperature, but instead directly from Eq. (7), again using the results of a separated calculation with non-gray walls for determining  $G_\eta$ .

### 3. PROBLEM DESCRIPTION AND NUMERICAL MODELING

The problem under study consists of a one-dimensional medium slab, as depicted in Fig. 1, bounded by two infinite, parallel, non-gray walls, separated by a distance  $L = 1$  m. The total pressure of the system is 1 atm and the participating medium is a homogeneous mixture of water vapor, carbon dioxide and a transparent gas, the former two with molar fractions of 0.2 and 0.1, respectively. A series of non-uniform temperature profiles is considered, all of them described by the following equation:

$$T(\hat{x}, x^*) = 400 \text{ K} \left[ 1 + \left( \frac{10}{x^*} \right) \hat{x} + \left( \frac{5}{x^{*2}} \right) \hat{x}^2 \right], \quad (13)$$

where  $\hat{x}$  is the dimensionless distance from the boundary on the left (cf. Fig. 1) and  $x^*$  is the value of  $\hat{x}$  corresponding to the maximum temperature within the domain. By increasing  $x^*$  from 0.5 (which yields a symmetrical, parabolic  $T$ -profile) to 1.0, the point of maximum temperature is gradually dislodged closer to the right-hand side boundary and the profile gets increasingly more asymmetrical. To illustrate this, Fig. 2(a) shows the resulting one-dimensional temperature profile for three different values of  $x^*$ .

For the radiative transfer solution, the RTE (either in its spectral or total form) is solved using the discrete ordinates method (Howell *et al.*, 2016). For this purpose, the domain is spatially discretized in 200 equal-sized cells and the directional integration of the RTE is performed for a total of 8 ordinates, adopting the set of weights and directional cosines provided by Lathrop and Carlson, 1964. Mesh quality analyses showed that these parameters are suitable for the study carried out in this paper.

The absorption spectra necessary for the LBL integration method are generated from the high-resolution spectral database HITEMP 2010 (Rothman *et al.*, 2010) at a resolution of  $0.067 \text{ cm}^{-1}$  and for a wavenumber range  $0 \text{ cm}^{-1} < \eta \leq 10\,000 \text{ cm}^{-1}$ , in which the spectrum was divided into 150 000 elements for both water vapor and carbon dioxide, adopting a Lorentz profile to describe the spectral line broadening. To save computational time, the spectral data is produced at constant 100 K-intervals, with temperatures varying from 400 K to 2500 K, and linearly interpolated for intermediary temperatures. Previous studies (Wang and Modest, 2004; Dorigon *et al.*, 2013; Cassol *et al.*, 2014) have shown that the spectral resolution and the other parameters presently adopted for generating the spectral data are sufficient for producing reliable results. More details about the LBL methodology employed here can be found in Dorigon *et al.*, 2013, and Coelho and França, 2018.

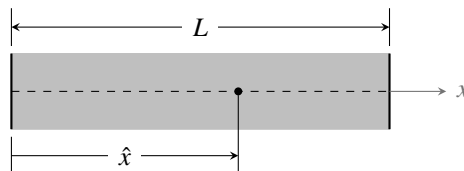


Figure 1. Geometry of the one-dimensional problem.

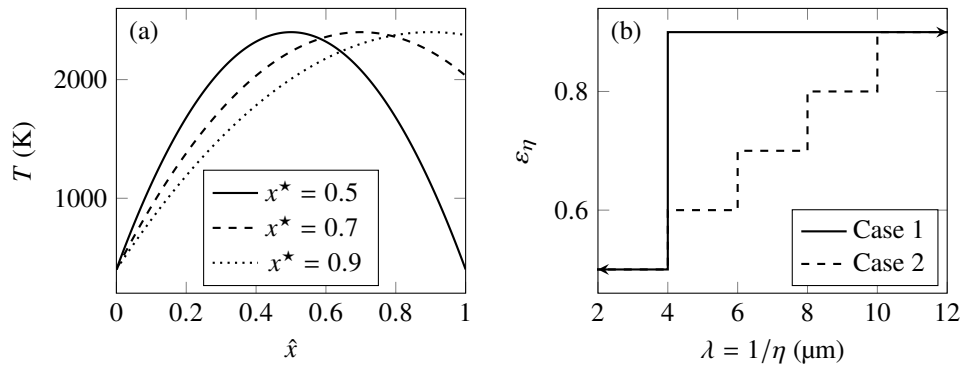


Figure 2. (a) Temperature profile for three distinct values of  $x^*$ ; (b) spectral emissivity profile with two and five spectral bands.

#### 4. RESULTS AND DISCUSSION

The reference to which the formulations of the GAA presented in section 2.3 of this paper are compared is obtained by a solution of the RTE in its spectral form, Eq. (1), considering truly non-gray boundary conditions, Eq. (2). Furthermore, a solution assuming the walls to be gray is also included, which is determined from Eqs. (3) and (4) with  $\alpha = \epsilon$ .

##### 4.1 Test case 1

The first test case studied in this paper considers that the walls that bound the medium are identical (i.e., with the same emissivity distribution) and have a two-interval stepwise  $\epsilon_\eta$ - $\eta$  relation, as shown by the solid line in Fig. 2(b). For convenience, this figure gives the spectral emissivity of the surface as a function of the wavelength  $\lambda$ , which is the inverse of  $\eta$ . The two constant emissivity values for test case 1 in Fig. 2(b) are  $\epsilon_\eta = 0.5$  for  $\lambda \leq 4 \mu\text{m}$ , and  $\epsilon_\eta = 0.9$  for  $\lambda > 4 \mu\text{m}$ .

For this case and three different temperature profiles (characterized by different values of  $x^*$ , see Eq. (13)), Fig. 3 plots the spatial distributions of the radiative heat flux,  $q_r$ , and the radiative heat source,  $S_r$ , obtained by the reference solution (actual non-gray treatment of the walls), by two different GAA formulations and by a solution considering the walls to be gray. The results of the other GAA formulations are omitted in the figure for brevity, but for all temperature profiles they tended to be very close to the GAA-4 solution.

For a symmetric temperature distribution,  $x^* = 0.5$ , all approaches provide a good approximation of the truly non-gray solution; considering the surfaces as gray, however, has errors of about 13 % for both  $q_r$  and  $S_r$ . As  $x^*$  increases and the temperature profile gets more asymmetrical, the discrepancies in relation to the reference solution get larger, as expected, particularly in the prediction of the radiative heat flux. For  $x^* = 0.7$ , Fig. 3 shows that the gray solution leads to significant

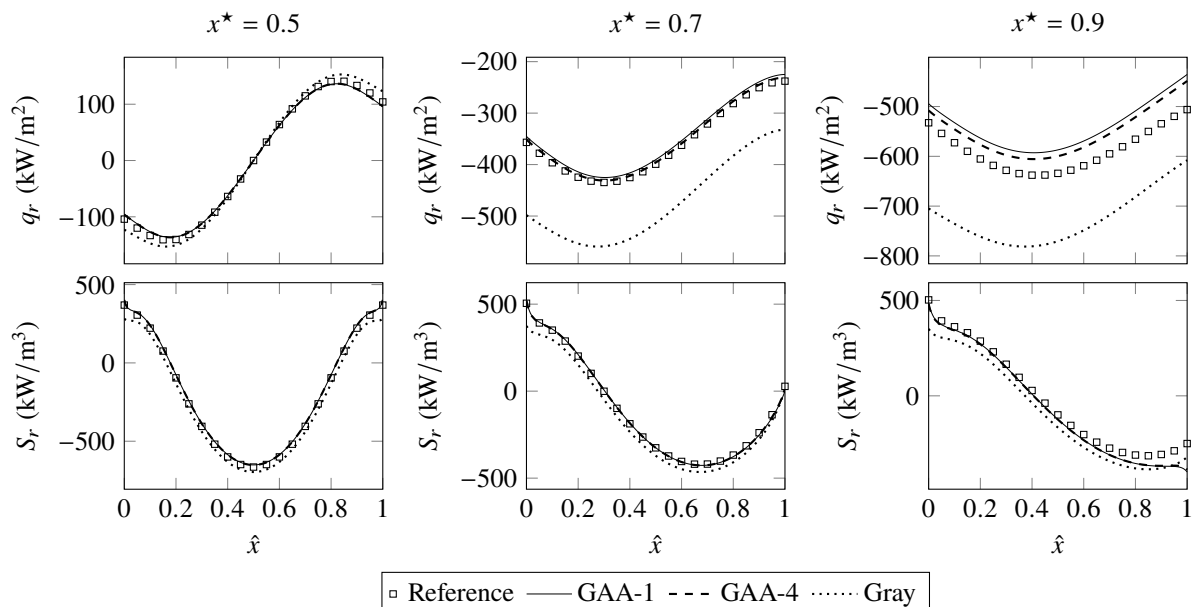


Figure 3. Radiative heat flux,  $q_r$ , and radiative heat source,  $S_r$ , over the domain for different values of  $x^*$  for Profile 1.

errors for  $q_r$  (the maximum error of this approach is above 30 %); conversely, both GAA formulations fair reasonably well, with errors of no more than 5 % (see Fig. 4). However, even the global absorptivity approach have non-negligible errors for  $x^* = 0.9$ , as depicted in the right-hand side of Fig. 3. Nonetheless, it is interesting to note that for this temperature profile the GAA-4 formulation, which adopts a transmissivity-weighted temperature average for determining  $T_{rm}$ , performs better than the simple domain-average approach (GAA-1) originally proposed by Fonseca *et al.*, 2018a.

To assess the performance of each solution, a normalized deviation from the reference solution can be defined as

$$\Delta\phi = \frac{|\phi_{\text{ref}} - \phi_{\text{app}}|}{\max(|\phi_{\text{ref}}|)}, \quad (14)$$

in which  $\phi$  is either the radiative heat flux or the radiative heat source, the subscripts “ref” and “app” indicate the reference solution and an approximate one, respectively, and  $\max(|\phi_{\text{ref}}|)$  is the maximum absolute local value of  $\phi_{\text{ref}}$  in the domain. The left-hand side of Fig. 4 reports the domain-averaged values of  $\Delta q_r$  and  $\Delta S_r$  for  $x^*$  ranging between 0.5 and 1.0 for all GAA formulations tested in this study. The normalized deviation of the gray solution is not shown in the figure because it is in general much larger than the ones of the GAA methods. This figure corroborates the previously discussed behavior of the errors associated to the GAA, which in general increase as the temperature profile gets more asymmetrical no matter how the presumed total absorptivity is calculated. Moreover, the errors in the prediction of the radiative heat flux tend to be larger than those of the radiative heat source, although this difference gets less significant with increasing  $x^*$ . Figure 4 also shows that there is a point of minimum (average) error around  $x^* = 0.7$ , where both  $(\Delta q_r)_{\text{avg}}$  and  $(\Delta S_r)_{\text{avg}}$  get below 2 %; currently there is no explanation available for this finding.

Comparing the different GAA formulation, note that, starting from  $x^* \approx 0.7$ , the GAA-1 solution has some of the largest errors, especially for  $q_r$  (for  $S_r$ , all approaches except for GAA-5 behave very similarly across all values of  $x^*$ ). This gives a strong indication that taking the reference medium temperature as the domain-average  $T$  when applying the GAA is not adequate for media with asymmetric temperature distributions; however, even in this approach, the average deviations from the reference solution do not exceed 8 %, which is well in the range of errors of some global models (Chu *et al.*, 2016, 2017; Centeno *et al.*, 2018). Curiously, the GAA-5 solution, where the presumed  $\alpha$  is the exact total hemispherical absorptivity (Eq. (6)) computed from the non-gray calculation, has the largest errors for  $q_r$  among all GAA formulations (for  $x^* > 0.65$ ), while having the smallest ones for  $S_r$ . Comparing the formulations where  $T_{rm}$  is calculated from a transmissivity-weighted average (GAA-2 to GAA-4), while all of them perform very similarly in terms of  $S_r$ , for  $q_r$  the GAA-3 solution slightly outperforms the GAA-4 one, and both of them have smaller errors than the GAA-2 formulation. This is surprising, seeing that the latter approach likely provides the most accurate prediction of the medium transmissivity, but is also positive in a practical sense, since evaluating  $\tau_{0 \rightarrow x}$  with Eq. (11) (as in GAA-2) is not feasible in calculations with global gas models; conversely, both GAA-3 and GAA-4 use an expression for the transmissivity (Eq. (12)) that is convenient and easily applicable to any global model.

The two upper plots in Fig. 5 depict the presumed absorptivity as calculated by each GAA-formulation for the left and right walls that bound the medium. Absorptivities estimated by the GAA-1 to GAA-4 formulations have a similar dependence on  $x^*$ , but their relative magnitude changes from the left to the right walls—i.e., for example, the GAA-3 methodology yields the largest  $\alpha$  at the left boundary and the smallest at the right one. Note also that  $\alpha$  calculated by

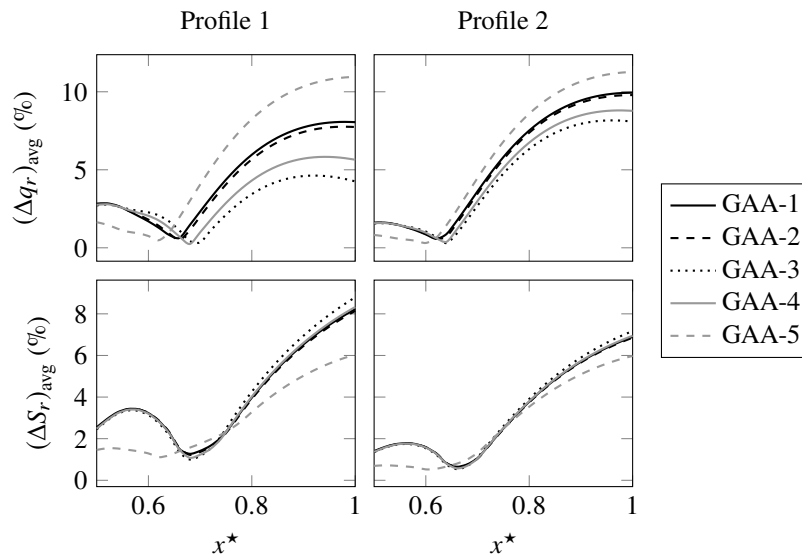


Figure 4. Domain-averaged normalized differences between the reference solution and each approach studied for Profile 1 (left) and Profile 2 (right).

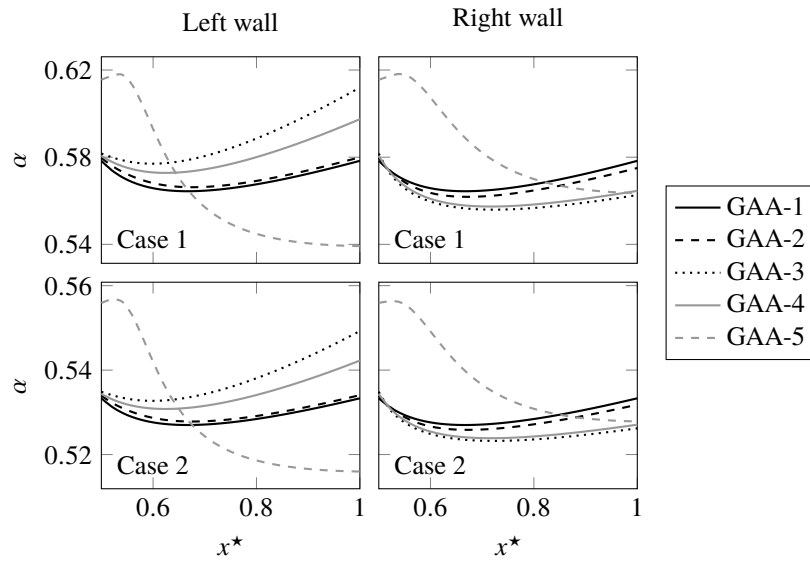


Figure 5. Total presumed absorptivity of left and right walls that bound the medium as predicted by the GAA formulations for different values of  $x^*$ .

GAA-1 is equal for both walls for any  $x^*$ , since  $T_{rm}$  has the same value for the two walls. The behavior of  $\alpha$  predicted by GAA-5 is different, decreasing with the increasing of  $x^*$  (while, for the other formulations,  $\alpha$  increases alongside  $x^*$ ). This solution is the most accurate for  $x^* < 0.65$ , (see Fig. 4), which is the  $x^*$ -range where GAA-5 predicts a significantly larger  $\alpha$  than the other formulations, for both left and right walls. This indicates that for  $x^* < 0.65$  the absorptivities to be used in the GAA methodology should be greater than what is computed via either Eq. (8) or Eq. (9).

A possible correction for that may lie on the total hemispherical emissivity of the boundaries. This quantity is plotted for the two walls in Fig. 6, again as a function of  $x^*$ . Note that the emissivity of the left surface is constant, approximately equal to 0.892 for case 1 and 0.804 for case 2, since the temperature that wall is always kept at 400 K. Moreover, for  $x^* < 0.6$ ,  $\varepsilon$  of the right wall is also quite large (since the wall temperature increases as the value of  $x^*$  grows), and greater than the presumed  $\alpha$  of any GAA formulation (compare Figs. 5 and 6). Therefore, it is possible that a new formulation for the GAA that, besides an average over the thermodynamical conditions of the medium, also takes into account the emissivity of the boundaries (or, equivalently, their temperature) to determine a value for  $\alpha$ , would improve the accuracy of the method. This shall be investigated in a future work.

#### 4.2 Test case 2

A second, more complex spectral emissivity profile is also considered in this study. Keeping all other conditions (e.g., medium composition and temperature profiles, total pressure) the same as test case 1, the walls are now assumed to have a five-interval stepwise  $\varepsilon_\eta$  distribution, represented by the dashed line in Fig. 2(b). These emissivity intervals are  $\varepsilon_\eta = 0.5$ , for  $\lambda < 4 \mu\text{m}$ ;  $\varepsilon_\eta = 0.6$ , for  $4 \mu\text{m} < \lambda < 6 \mu\text{m}$ ;  $\varepsilon_\eta = 0.7$ , for  $6 \mu\text{m} < \lambda < 8 \mu\text{m}$ ;  $\varepsilon_\eta = 0.8$ , for  $8 \mu\text{m} < \lambda < 10 \mu\text{m}$ ; and  $\varepsilon_\eta = 0.9$ , if  $\lambda > 10 \mu\text{m}$ .

The results for this case follow the same trend as case 1. The right-hand side of Fig. 4 shows the domain-averaged values of the normalized difference  $\Delta$  between each GAA formulation and the reference solution as a function of  $x^*$  (once again, the gray solution yielded much larger errors than the GAA). Except for a narrow interval where  $x^* < 0.65$ , the GAA-3 solution outperforms the other for  $q_r$ , while GAA-5 is the best in predicting  $x^*$  for almost all temperature profiles.

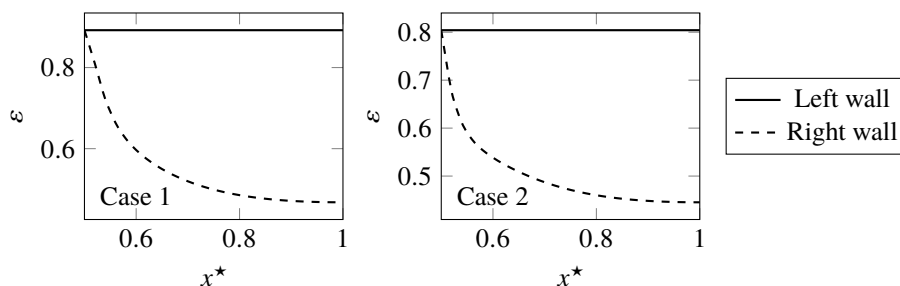


Figure 6. Total emissivity of the left and right walls for different values of  $x^*$ .

Nevertheless, for the radiative heat source the average error of the GAA-3 formulation is no more than 7%. The error of taking  $T_{rm}$  as the domain-average temperature increases as the temperature distribution gets less symmetric, being one of the greatest for  $x^* > 0.65$ .

Figure 5 shows that  $\alpha$  computed by the GAA formulations for different  $x^*$  have similar behaviors as the ones for case 1, although their values are smaller—the same can also be verified for the total emissivity, see Fig. 6. In this light, it is interesting to note that the decrease in  $\alpha$  and  $\varepsilon$  from case 1 to case 2 did not significantly alter the errors of each approach (compare the errors for those cases plotted in Fig. 4). However, this is likely because the spectral emissivity profiles of cases 1 and 2 are relatively similar, so a very different performance of the GAA (for better or worse) can be expected for other  $\varepsilon_\eta$ - $\eta$  relationships.

## 5. CONCLUSIONS

This study presented five manners of application of the global absorptivity approach to estimate the total absorptivity of a one-dimensional non-gray medium slab. Three of the methods were based on a domain-average of the temperature weighted by the transmissivity from any boundary to the medium, and their accuracy was compared to the original formulation of the GAA (which is based on a simple domain-average of the temperature) and to another approach in which the total hemispherical absorptivity is directly determined of the definition of  $\alpha$ . The test cases consisted of a homogeneous medium subjected to a series of increasingly asymmetric temperature profiles. The results showed that, as the temperature distribution got less symmetric, computing the absorptivity from a domain-average temperature is in general less accurate than a transmissivity-weighted average. However, the latter approach did not perform as well as the formulation that directly calculates  $\alpha$  from its definition—which, in turn, is not practical for applications to global gas models—for roughly symmetric profiles. Additionally, further analyses showed that a possible improvement to the GAA could come about by also taking into account the temperature of the boundaries when computing  $\alpha$ .

## 6. ACKNOWLEDGEMENTS

This work has been partially supported by the Brazilian agency CAPES. Authors RJCF and GCF thank CAPES and CNPq for their doctorate scholarships. FHRF also thanks CNPq for research grants 302686/2017-7.

## 7. REFERENCES

- Cassol, F., Brittes, R., Centeno, F.R., da Silva, C.V. and França, F.H.R., 2015. "Evaluation of the gray gas model to compute radiative transfer in non-isothermal, non-homogeneous participating medium containing CO<sub>2</sub>, H<sub>2</sub>O and soot". *Journal of the Brazilian Society of Mechanical Sciences and Engineering*, Vol. 37, No. 1, pp. 163–172. doi:10.1007/s40430-014-0168-5.
- Cassol, F., Brittes, R., França, F.H.R. and Ezekoye, O.A., 2014. "Application of the weighted-sum-of-gray-gases model for media composed of arbitrary concentrations of H<sub>2</sub>O, CO<sub>2</sub> and soot". *International Journal of Heat and Mass Transfer*, Vol. 79, pp. 796–806. doi:10.1016/j.ijheatmasstransfer.2014.08.032.
- Centeno, F.R., Brittes, R., Rodrigues, L.G.P., Coelho, F.R. and França, F.H.R., 2018. "Evaluation of the WSGG model against line-by-line calculation of thermal radiation in a non-gray sooting medium representing an axisymmetric laminar jet flame". *International Journal of Heat and Mass Transfer*, Vol. 124, pp. 475–483. doi:10.1016/j.ijheatmasstransfer.2018.02.040.
- Chu, H., Consalvi, J.L., Gu, M. and Liu, F., 2017. "Calculations of radiative heat transfer in an axisymmetric jet diffusion flame at elevated pressures using different gas radiation models". *Journal of Quantitative Spectroscopy and Radiative Transfer*, Vol. 197, pp. 12–25. doi:10.1016/j.jqsrt.2017.02.008.
- Chu, H., Gu, M., Consalvi, J.L., Liu, F. and Zhou, H., 2016. "Effects of total pressure on non-grey gas radiation transfer in oxy-fuel combustion using the LBL, SNB, SNBCK, WSGG, and FSCK methods". *Journal of Quantitative Spectroscopy and Radiative Transfer*, Vol. 172, pp. 24–35. doi:10.1016/j.jqsrt.2015.07.009.
- Coelho, F.R. and França, F.H.R., 2018. "WSGG correlations based on HITEMP2010 for gas mixtures of H<sub>2</sub>O and CO<sub>2</sub> in high total pressure conditions". *International Journal of Heat and Mass Transfer*, Vol. 127, pp. 105–114. doi:10.1016/j.ijheatmasstransfer.2018.07.075.
- Denison, M.K. and Webb, B.W., 1993. "A spectral line-based weighted-sum-of-gray-gases model for arbitrary RTE solvers". *Journal of Heat Transfer*, Vol. 115, No. 4, p. 1004. doi:10.1115/1.2911354.
- Denison, M.K. and Webb, B.W., 1994. "k-distributions and weighted-sum-of-gray-gases—a hybrid model". *Heat Transfer*, Vol. 2, pp. 19–24. doi:10.1615/IHTC10.4890.
- Dorigon, L.J., Duciak, G., Brittes, R., Cassol, F., Galarça, M. and França, F.H.R., 2013. "WSGG correlations based on HITEMP2010 for computation of thermal radiation in non-isothermal, non-homogeneous H<sub>2</sub>O/CO<sub>2</sub> mixtures". *International Journal of Heat and Mass Transfer*, Vol. 64, pp. 863–873. doi:10.1016/j.ijheatmasstransfer.2013.05.010.
- Fonseca, R.J.C., Fraga, G.C. and França, F.H.R., 2018a. "A simplified approach to compute the radiative transfer in a

- participating medium bounded by non-gray walls”. In *Proceedings of the Eurotherm Seminar 110—Computational Thermal Radiation in Participating Media - CTRPM 2018*.
- Fonseca, R.J.C., Fraga, G.C., Silva, R.B. and França, F.H.R., 2018b. “Application of the WSGG model to solve the radiative transfer in gaseous systems with nongray boundaries”. *Journal of Heat Transfer*, Vol. 140, No. 5, pp. 052701–1. doi:10.1115/1.4038548.
- Howell, J.R., Mengüç, M.P. and Siegel, R., 2016. *Thermal Radiation Heat Transfer*. CRC press, 6th edition.
- Lathrop, K.D. and Carlson, B.G., 1964. “Discrete ordinates angular quadrature of the neutron transport equation”. Technical report. doi:10.2172/4666281.
- Modest, M.F., 1991. “The weighted-sum-of-gray-gases model for arbitrary solution methods in radiative transfer”. *Journal of Heat Transfer*, Vol. 113, No. 3, pp. 650–656. doi:10.1115/1.2910614.
- Modest, M.F., 2013. *Radiative Heat Transfer*. Academic Press.
- Rothman, L., Gordon, I., Barber, R., Dothe, H., Gamache, R., Goldman, A., Perevalov, V., Tashkun, S. and Tennyson, J., 2010. “HITEMP, the high-temperature molecular spectroscopic database”. *Journal of Quantitative Spectroscopy and Radiative Transfer*, Vol. 111, No. 15, pp. 2139–2150. doi:10.1016/j.jqsrt.2010.05.001.
- Silva, R.M., Fonseca, R.J.C. and França, F.H.R., 2018. “Radiative transfer prediction in participating medium bounded with nongray walls using SLW model”. In *Proceedings of the 17th Brazilian Congress of Thermal Sciences and Engineering—ENCIT 2018*.
- Solovjov, V.P., Lemmonier, D. and Webb, B.W., 2013. “Efficient cumulative wavenumber model of radiative transfer in gaseous medium bounded by non-gray walls”. *Journal of Quantitative Spectroscopy & Radiative Transfer*, Vol. 128, pp. 2–9. doi:10.1016/j.jqsrt.2012.07.017.
- Wang, A. and Modest, M.F., 2004. “Importance of combined Lorentz-Doppler broadening in high-temperature radiative heat transfer applications”. *Journal of Heat Transfer*, Vol. 126, No. 5, p. 858. doi:10.1115/1.1798951.

## 8. RESPONSIBILITY NOTICE

The authors are solely responsible for the printed material included in this paper.